ADVANCED ENGINEERING MATERIALS
www.aem-journal.com

Bioinspired Hydrophilic and Oleophilic Absorption Media from Biotemplated Fungi

Debora Lyn Porter, Hammad Malik, Casey Elliott, Krista Carlson, and Steven E. Naleway*

Fungi are an incredibly diverse biological kingdom with organisms that have a wide range of morphologies, properties, and structures. Previous research has investigated the use of filamentous fungi, which have naturally porous structures created by hyphal filaments, as a means of phytoremediation. This study uses these natural fungal structures to create bioinspired materials that capture both the structure and functional absorption properties of fungi. Three types of filamentous fungi with different hyphal structures (monomitic, dimitic, and trimitic) are used as organic templates to create inorganic media using two different biotemplating methods to create silica and hybrid samples. Characterization of these samples is completed using scanning electron microscope imaging, chemical characterization, nanoindentation, and hydrophilic and oleophilic absorption tests. Biotemplated samples have similar structures as their organic templates, but contained silica, which is not present in natural, dehydrated fungal samples. Fourier transform infrared analysis shows better cross-linking in the hybrid samples, which also have higher mechanical resistance than the silica samples. Absorption testing demonstrates that silica samples are closest to mimicking the absorption properties of natural, dehydrated samples. Of the three hyphal structures, the monomitic samples show the greatest increase in mechanical properties and maintenance of absorption properties when biotemplated.

1. Introduction

Fungi is an incredibly diverse biological kingdom that continues to be discovered and described, with organisms that range from sporocarp (mushroom) forming species to molds, rusts, and smuts. The abundance of the organisms classified as fungi offers many research avenues, with thousands of new species discovered each year.[1–3] Recent research has reflected a growing interest in studying fungal biomechanics[4–10] and characterizing the mechanical and material properties of different fungi and their various structures.[11–15] This better understanding of fungi and their properties has led to a growing interest in incorporating fungi into engineering materials and applications, including creating more environmentally friendly packaging materials, construction materials, and fabrics.[16–18] However, the use of fungi as an engineering material is limited due to its natural material and mechanical properties. The ability to adjust and tailor the properties of the natural structure of fungi, whose primary constituent is chitin,[19] could allow for the integration of these structures into applications where the material and mechanical properties of fungi would not be suitable.

Perhaps most intriguing among the beneficial properties of filamentous fungi is their naturally porous structure, which makes the structures suitable for applications such as absorption or filtration. In their natural environment, fungi are known to be hydrophilic, giving them an advantage in absorbing water to achieve the hydration necessary to survive and reproduce.[20] Additionally, fungi are able to absorb a variety of natural and man-made impurities like heavy metals or other elemental contaminants in their environment.[21,22] This ability to aid in phytoremediation makes fungi an excellent choice for bioinspiration. While fungi-aided phytoremediation largely depends on the biochemistry of the fungi, the filamentous structure characteristic of filamentous fungi, such as those in the *Agaricomycetes* class of fungi, lends itself to absorption of liquids through mechanisms like capillary action.[23] Thus, fungi can act as a source of bioinspiration in the creation of materials that can aid in environmental remediation in absorbing or filtering liquids such as oil.

One way the natural structures of fungi could be incorporated into engineered materials is the use of biotemplating. Biotemplating is a manufacturing technique by which biological structures can be copied into inorganic materials at various length scales.[24,25] This process begins by taking the natural material that will act as the organic template, such as fungi, and chemically breaking down the biological constituents.

D. L. Porter, S. E. Naleway
Department of Mechanical Engineering
The University of Utah
1495 E 100 S, Salt Lake City, UT 84112, USA
E-mail: deboralyn.porter@utah.edu

H. Malik, C. Elliott, K. Carlson
Reno Department of Chemical and Materials Engineering
University of Nevada
1664 N Virginia St., Reno, NV 89557, USA

The ORCID identification number(s) for the author(s) of this article can be found under https://doi.org/10.1002/adem.202200945.

DOI: 10.1002/adem.202200945

Next, the inorganic material is deposited or infiltrated into the organic template. The biotemplating process is completed by removing the organic template, leaving an inorganic copy of the chosen natural structure.[24–29] The chemicals typically used in biotemplating are corrosive or toxic, which limits the researchers using them on natural materials with greater chemical toughness, such as wood or pinecones, which are robust enough to withstand the degradation of the organic template during this harsh process due to their content of lignin, which provides a tougher, more chemically resistant structure.[25,26,30] Recently, other biotemplating methods have been developed to template more delicate materials such as celery[31] or fungi.[29] The mechanical and absorption properties of these biotemplated copies, which use a more delicate organic template and more environmentally friendly chemical processes, are still largely unknown.

This study characterizes the structure, mechanical properties, material properties, and hydrophilic/oleophilic absorption properties of biotemplated copies of three types of representative *Agaricomycetes* fungal structures (monomitic, dimitic, and trimitic hyphal systems) using two different biotemplating methods to modulate these properties. The properties of these biotemplated copies were tailored using two biotemplating methods to create a silica sample and a silica-chitin hybrid sample, which both maintain some degree of the hydrophilic/oleophilic absorption properties found in the natural fungal structures. Characterization was performed using imaging, nanoindentation, chemical analysis, and absorption testing to understand how incorporating both the microstructure and biotemplating method can tailor the properties of these porous, inorganic materials to create fungi-inspired environmental remediation materials. This understanding will advance the current knowledge of how fungal structures can be biotemplated and how the beneficial properties of fungi can be harnessed to address current environmental issues such as oil-contamination remediation.

2. Experimental Section

2.1. Organic Template Selection and Preparation

Three *Agaricomycetes* fungal sporocarps were used as organic templates to study the differences in properties of the biotemplated fungal samples based on their microstructure (**Figure 1**). All *Agaricomycetes* fungi can be classified by their constituent material, hyphae, which come in three different varieties: generative, skeletal, and ligative hyphae. White mushrooms (*Agaricus bisporus*)[32–34] were selected for their monomitic structure, having only generative hyphae. Maitake mushrooms (*Grifola frondosa*)[32,35,36] were chosen for their dimitic structure, having both generative and skeletal hyphae. Reishi mushrooms (*Ganoderma lingzhi*)[32,37–39] were chosen for their trimitic structure, having generative, skeletal, and ligative hyphae. These three types of fungal sporocarps have been studied in previous work, which allows for direct comparison.[15] In addition, despite having the same basic constituents, fungal sporocarps with different hyphal structures have different morphologies, structures, mechanical properties, and levels of hydration.[15,20] Fresh white and maitake mushroom sporocarps and a dehydrated reishi sporocarp were acquired from local retailers. To keep fungal cells inflated, which promotes better fluid exchange, sporocarp samples were templated in a hydrated state. To achieve this consistent hydration, dehydrated samples were rehydrated by being soaked in 3 wt% hydrogen peroxide for 48 h to achieve better hydration of the samples.[40] While hydrogen peroxide is known to slow the growth of fungi and can cause death in live fungi,[41,42] research has shown that treatment with hydrogen peroxide does not cause significant structural damage to the microstructure of fungal sporocarps as compared to sporocarps treated with water.[43]

2.2. Biotemplating

Two methods of biotemplating were used to make the biotemplated samples (**Figure 2**). The first method involved soaking hydrated sporocarp samples in tetraethyl orthosilicate (TEOS, reagent grade, 98%, Sigma-Aldrich, St. Louis, MO, USA) for 48 h and then calcining in a Thermo Scientific Thermolyne furnace (Thermo Fisher Scientific, Waltham, MA, USA) for 2 h at 500 °C. Because of the use of a silica precursor and the calcining process, burning off organic material, these samples will be referred to as "silica" samples hereafter. The second method involved soaking hydrated sporocarp samples first in acetic acid (1% v/v aqueous solution, Thermo Fisher Scientific) for 48 h to break down the chitin, rinsing them in water to remove the remaining acetic acid, and then soaking them in TEOS for 48 h. Following the acetic acid and TEOS treatments, the samples were allowed to air dry at room temperature for 48 h, during

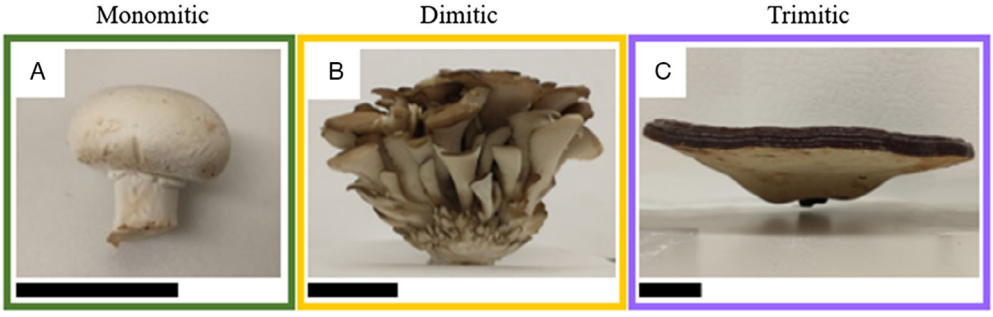

Figure 1. Images of the monomitic, dimitic, and trimitic sporocarps used in this study to make dehydrated, silica, and hybrid samples. Representative sporocarps include: A) white mushrooms, B) maitake mushrooms, and C) Reishi mushrooms. Scale bars represent 4 cm.

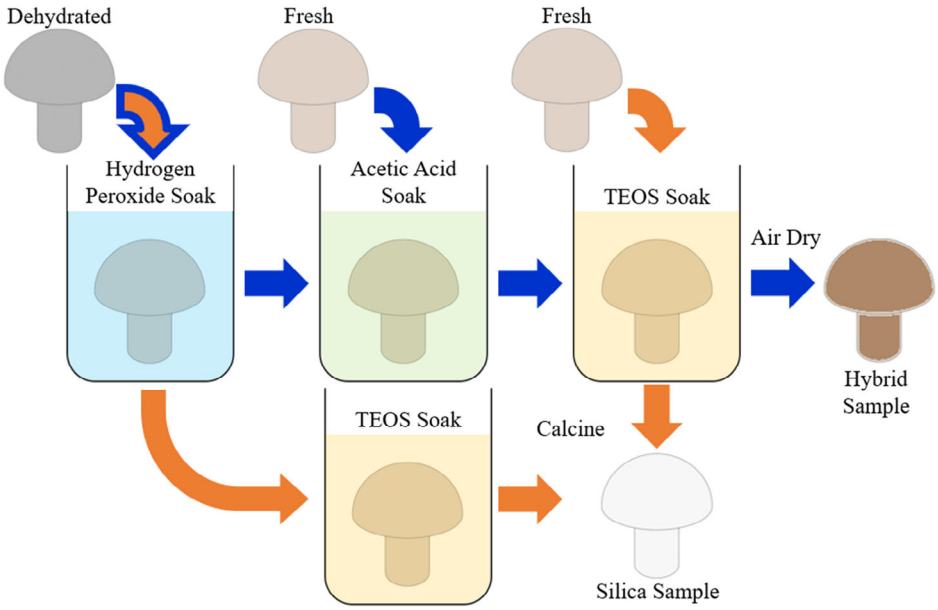

Figure 2. The biotemplating processes used to create silica and silica-chitin hybrid samples. The process for creating silica samples can be seen by following the orange arrows and the process for creating hybrid samples can be seen by following the blue arrows.

which time the change in pH induced by the acetic acid catalyzes the TEOS into silica. Because the organic template was not fully removed in this process, these silica-chitin hybrid samples will be referred to as "hybrid" samples hereafter. Both biotemplating methods were adapted from previous work[30,31] but had not previously been applied to fungi, nor other chitinous materials. To compare biotemplated samples with their organic templates, dehydrated samples were made by placing fresh sporocarp samples in a Magic Mill® food dehydrator (Royalux Inc., Spring Valley, NY, USA) for 10 h at 40 °C. For characterizing and comparing the properties, all three types of samples (dehydrated, silica, and hybrid) for each of the monomitic, dimitic, and trimitic hyphal structures were used.

2.3. Structural Imaging

Imaging samples were made and imaged to analyze the structure of biotemplated and dehydrated samples. Three imaging samples each were made by sectioning pieces with a cross-sectional area of ≈10 mm^2 from the dehydrated, silica, and hybrid samples of monomitic, dimitic, and trimitic sporocarps. Samples were then fixed to aluminum sample holders with carbon tape and coated with ≈20 nm of gold-palladium. Images of the samples were taken using an FEI Quanta 600FE-ESEM scanning electron microscope (SEM, Hillsboro, OR, USA) at an accelerating voltage of 5 kV and spot size of 3 nm. Image analysis of the similarity of the microstructures of the different types of samples was done using ImageJ by measuring the hyphal filaments and the porosity of the structures. This was done by taking two representative images from each type of sample and overlaying ellipses over the hyphal filaments, the solid filaments that shape the porous structure, and measuring the aspect ratio (the length of the major axis divided by the minor axis). For each image, a minimum of 42 measurements were taken, for a minimum of 84 hyphal measurements for each type of sample. Because of the samples' hydrophilicity, it was not possible to perform porosity measurements using Brunauer–Emmett–Teller (BET) method. Instead, the overall porosity of the internal structures was measured with ImageJ using two representative images taken for each type of hyphal system (monomitic, dimitic, trimitic) for each type of sample (dehydrated, silica, hybrid). Each porosity image provided one measurement, meaning that each type of sample had two porosity measurements.

2.4. Chemical Composition

While samples were in the SEM, energy dispersive X-ray spectroscopy (EDS) was performed using APEX EDS Software (EDAX Inc., Mahwah, NJ, USA). Elemental maps, generated using the EDS software, were completed on the surface of each type of sample (dehydrated, silica, and hybrid) of each type of sporocarp (monomitic, dimitic, and trimitic). EDS was completed using an accelerating voltage of 20 kV and a spot size of 4.0 nm. Image outputs were adjusted to remove the elements present due to coating the imaging samples (i.e., gold and palladium).

The chemical compositions of the two biotemplated sample types, silica and hybrid, were compared using FTIR analysis. A single FTIR sample was used for each type of sample tested, resulting in a total of six spectra. Representative FTIR spectra were collected for silica and hybrid samples of the monomitic, dimitic, and trimitic hyphal systems using a Thermo Scientific Nicolet 380 equipped with OMNIC software (Thermo Fisher Scientific). To collect each spectrum, the

FTIR sample was placed onto a clean, diamond-tipped attenuated total reflection (ATR) window and pressed using the pressure tower. All measurements were collected in ambient conditions, with the scan range for all samples set between 400 and 4000 cm^{-1}.

Thermogravimetric analysis (TGA) was used to further quantify differences in the composition between the dehydrated, silica, and hybrid samples. Monomitic samples of each type were prepared by crushing each type of sample (dehydrated, silica, and hybrid) until there was between 10 and 20 mg of crushed sample. TGA was performed using a Netzsch Simultaneous Thermal Analyzer (STA) 449F3 (NETZSCH -Gerätebau GmbH, Selb, Germany). Crushed samples were added to the thermal analyzer for testing and analysis after a baseline correction was completed for each sample. Samples were tested from 20 to 500 °C using a ramp rate of 20 °C min^{-1}.

2.5. Mechanical Testing

Mechanical testing was completed using nanoindentation. Mechanical testing samples were prepared by taking sections of each type of sample (dehydrated, silica, and hybrid), roughly 3.5 mm^2 in cross-sectional area, for each of the monomitic, dimitic, and trimitic sporocarp samples. These mechanical testing samples were fixed on 15 mm diameter specimen discs (Ted Pella, Redding, CA, USA) with cyanoacrylate glue. Nanoindentation was completed using a Hysitron TI Premier Nanoindenter system (Hysitron Inc., Minneapolis, MN, USA) using a Berkovich diamond tip probe. The load function was set up as a trapezoidal function with a maximum load of 500 μN. Each mechanical testing sample was indented in 5 different locations, each at least 1 μm from the other, for a total of 45 nanoindentation locations across all types of samples.

2.6. Hydrophilic and Oleophilic Absorption Testing

The functional properties of the biotemplated samples were tested by completing absorption testing. Fungal sporocarps are known to be hydrophilic, though the exact water content of the sporocarp depends on its environment, species, and age.[20] Absorption samples were created for each type of sample (dehydrated, silica, and hybrid) for each of the types of hyphal systems (monomitic, dimitic, and trimitic). Four replicates were made of each absorption sample for each test (**Figure 3**), meaning a total of 36 samples were used in each absorption test. The mass of each absorption sample was measured to get a dry mass measurement. The replicate was then placed into a liquid for 15 min. At the end of 15 min, the absorption sample was removed from the liquid and the mass was again measured to determine how much liquid was absorbed. Absorption was determined by dividing the final weight of the absorption samples by their dry weight. Two different tests were performed using this method: the first test used water to test the hydrophilicity, and the second used soybean oil to test the oleophilicity. The average absorption of each type of absorption sample was then calculated for each test.

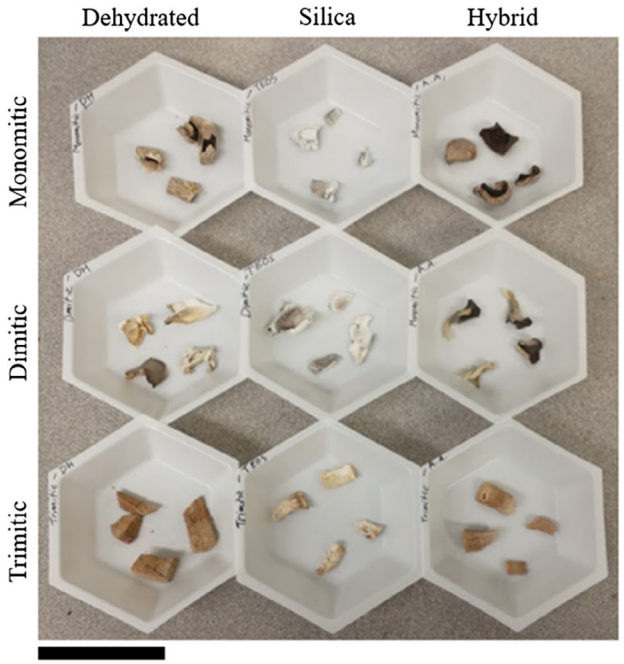

Figure 3. Representative absorption samples used prior to a liquid absorption test. The scale bar represents 5 cm.

2.7. Statistical Analysis

Statistical analysis was completed using one-way analysis of variance (ANOVA) tests. ANOVA tests were performed using MATLAB (MathWorks, Natick, MA, USA). When a significant difference was observed, pairwise comparisons were performed using Tukey's honest significant difference (HSD). In the case of comparing the aspect ratio of the filaments seen in the microstructure (see Section 2.3 Structural Imaging), because the data was heavily skewed, a logarithmic transformation was used to transform the data to be normally distributed before running ANOVA and Tukey HSD tests. A significance level of $\alpha = 0.05$ was used for all tests to determine significance.

3. Results and Discussion

3.1. Structural Analysis

Loosely packed hyphal systems were visible in the SEM images taken of the monomitic, dimitic, and trimitic samples (**Figure 4**). The hyphae are most clearly seen in the dehydrated samples, where the hyphae have experienced no processing (Figure 4A,D,G). The structures created by these hyphal systems are similar to the silica samples (Figure 4B,E,H). While hyphal filaments are visible in the hybrid samples, there appears to be a greater degree of fusion between the hyphal filaments (Figure 4C,F,I). The trimitic biotemplated samples showed both the hyphal filaments, and the tubular mesostructure typical of reishi mushrooms (Figure 4H, I).[15] For each type of hyphal structure, the hyphal filaments that make up the microstructure of the dehydrated, silica, and hybrid samples had an average aspect ratio of ≈3. There were

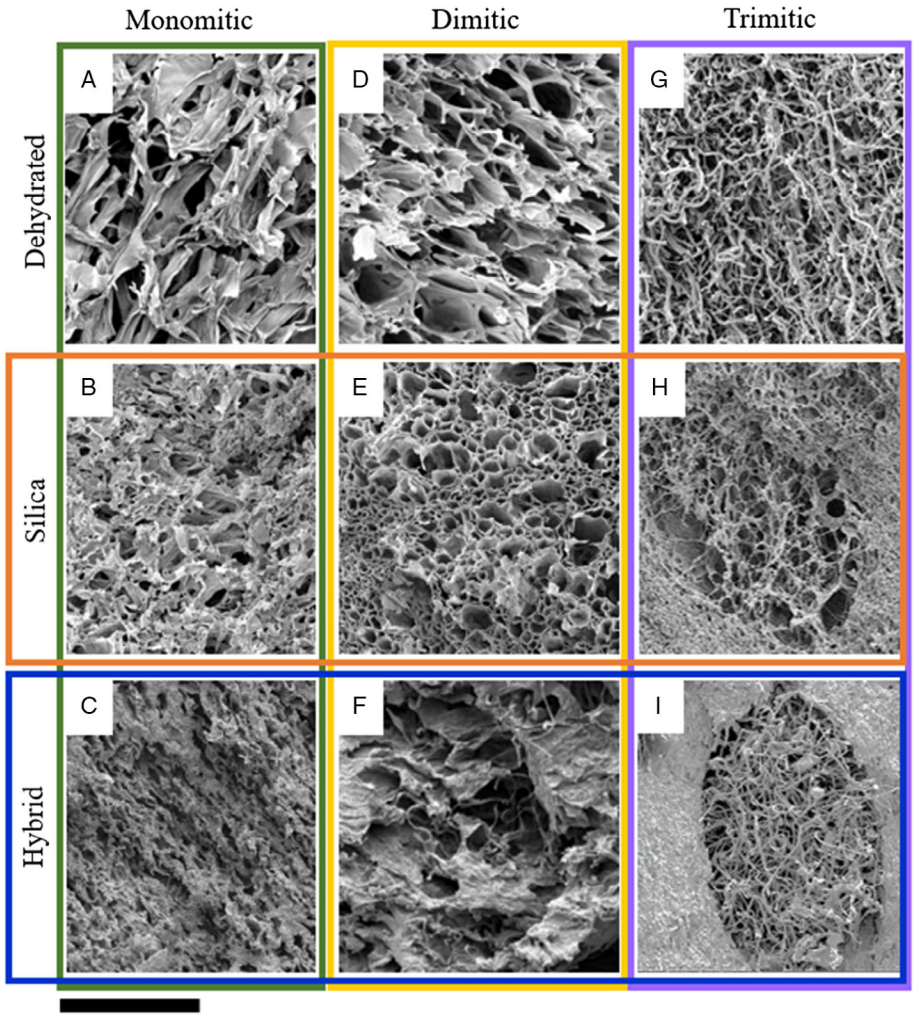

Figure 4. Representative scanning electron microscope (SEM) images for the A–C) monomitic, D–F) dimitic, and G–I) trimitic samples of each type (dehydrated, silica, and hybrid). Images show the filamentous hyphal systems that create the larger structures. The scale bar represents 100 μm.

no statistically significant differences ($p \geq 0.06$) in the different types of samples with the same microstructures (monomitic, dimitic, trimitic) suggesting that the filaments present in the dehydrated samples are replicated in the silica and hybrid samples.

Though the basic structure and dimensions of the hyphal systems were captured in the silica and hybrid samples, there was a change in the porosity of the samples when compared to the dehydrated sporocarps. The average porosity of each type of sample is found in **Table 1**. For each of the hyphal systems (monomitic, dimitic, and trimitic), there was a decrease in the porosity of the microstructure when comparing the dehydrated samples to both the silica and hybrid samples, with the largest decrease in porosity occurring in the hybrid samples. While there were no statistically significant differences in the porosity between the silica and hybrid samples, there were differences in porosity that were statistically significant when comparing the dehydrated monomitic and dimitic samples to their respective silica and hybrid samples with p values all less than $p = 0.02$. While the average porosity decreased with the trimitic samples, there were

Table 1. The average porosity ($N = 2$ for each) of the monomitic, dimitic, and trimitic hyphal systems with their different types of samples (dehydrated, silica, and hybrid) along with the reduction in porosity, as compared to the average porosity in dehydrated samples, that results from each biotemplating process. Matching Greek letters next to the porosity values indicates a statistically significant difference.

Hyphal System	Type	Porosity [%]	Reduction in Porosity [%]
Monomitic	Dehydrated	$27.2 \pm 0.8^{\alpha,\beta}$	0
	Silica	$23.2 \pm 0.1^{\alpha}$	14.9
	Hybrid	$21.2 \pm 0.2^{\beta}$	22.0
Dimitic	Dehydrated	$27.2 \pm 0.8^{\gamma,\delta}$	0
	Silica	$21.5 \pm 0.3^{\gamma}$	21.0
	Hybrid	$19.4 \pm 0.7^{\delta}$	28.7
Trimitic	Dehydrated	26.4 ± 1.1	0
	Silica	20.6 ± 0.3	22.1
	Hybrid	18.2 ± 2.8	31.2

no statistically significant differences. This larger reduction in porosity can also be seen in the representative SEM images (Figure 4C,F,I). The monomitic silica and hybrid samples showed the smallest overall decrease in porosity when compared to the monomitic dehydrated samples, with a reduction in porosity of 14.9% and 22.0% for the silica and hybrid samples, respectively. The silica samples for both the dimitic and trimitic samples had a reduction in porosity of just over 20%, and the hybrid samples had a reduction in porosity of closer to 30%. This trend in the reduction in porosity from the dehydrated samples to the silica and hybrid samples suggests that the biotemplating methods used in this study result in a less porous structure than natural dehydrated samples, though the general microstructure of the samples is maintained.

The microstructure of the hyphal systems, as seen in SEM images (Figure 4), can be successfully mimicked using the biotemplating techniques used in this work. Sol–gel processes can use silica precursors, which then allow crosslinking of silica chains to form on the nanoscale.[44] By using fungal sporocarps as an organic template, the biotemplated samples introduce a microstructure: the hyphal systems. While the internal structure of the biotemplated samples did change, leading to less porous samples, this added density may increase the mechanical resistance of the samples without affecting the absorption properties of the natural structure.

3.2. Chemical Analysis

Data from elemental mapping, performed using EDS, showed a change in the elemental composition between the dehydrated and biotemplated samples (**Figure 5**). **Table 2** shows the weight percentages of the main elements found in each of the samples. All the dehydrated samples (monomitic, dimitic, trimitic) are primarily made up of carbon and oxygen, though some trace elements were also present in the monomitic and dimitic samples. This is consistent with other organic materials, including other fungi.[11] All the biotemplated samples included some weight percent of silicon, and maintained relatively high levels of oxygen, indicative of the presence of silica. The silica samples had the highest weight percent of silicon, with all three hyphal types achieving higher than 32 wt%. This presence of relatively high amounts of silicon in the silica samples was accompanied

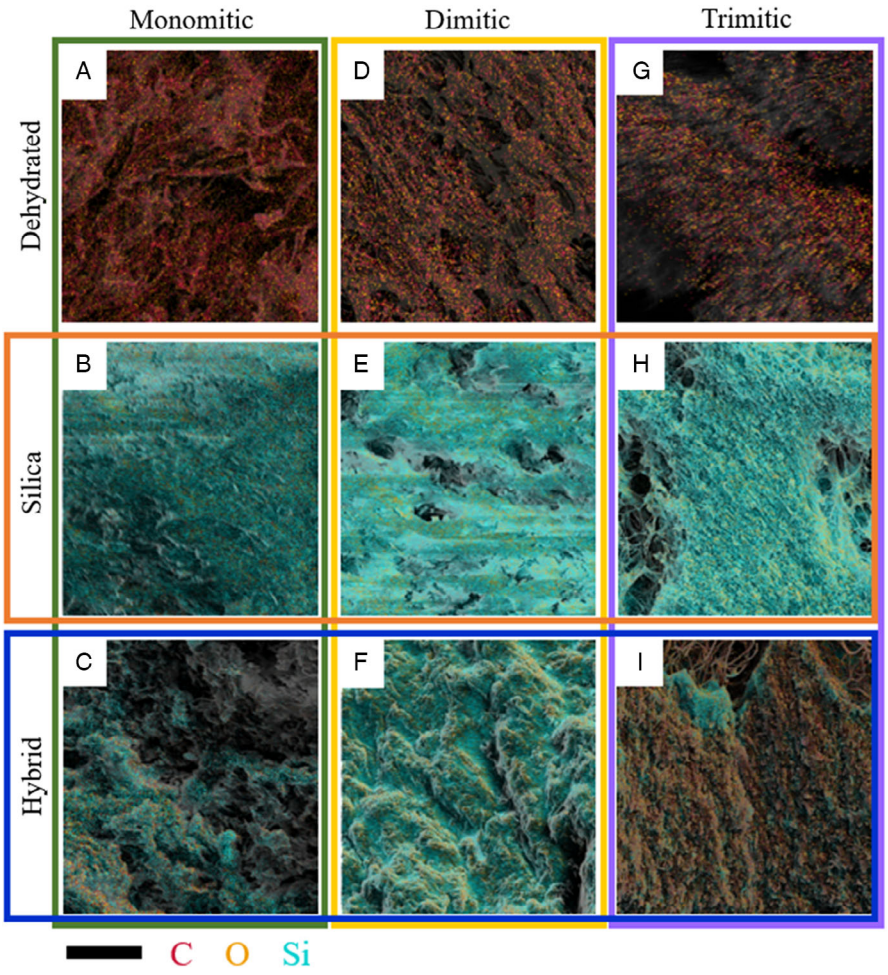

Figure 5. Representative energy dispersive X-ray spectroscopy (EDS) maps of: A–C) monomitic, D–F) dimitic, and G–I) trimitic samples of each type (dehydrated, silica, and hybrid). Trace elements are not included in the maps, showing only the most abundant elements (carbon, oxygen, and silicon). The scale bar represents 50 μm.

Table 2. Elemental weight percentages of C, O, and Si found on samples using EDS. Note that trace elements for the samples are not listed, so the wt% of each does not necessarily add to 100%.

Hyphal System	Element	Dehydrated [wt%]	Silica [wt%]	Hybrid [wt%]
Monomitic	C	41.8	6.3	44.3
	O	45.5	45.6	39.1
	Si	0	34.5	9.1
Dimitic	C	45	0	28.4
	O	41.2	51.2	48.4
	Si	0	44.1	18.8
Trimitic	C	51.4	10.8	47.9
	O	48.6	46.4	47.9
	Si	0	36.0	9.2

by a sharp decrease in the amount of carbon detected. In contrast, the hybrid samples all maintained higher levels of carbon while still including significant concentrations of silicon (less than 20 wt% for all samples).

EDS mapping showed that the silica and hybrid samples both had the addition of silicon, which was not found in the dehydrated samples (Figure 5, Table 2). The inclusion of silicon and oxygen suggests the presence of silica, which was expected from using a silica precursor. The higher levels of carbon in the hybrid samples may indicate the presence of chitin, which is the main constituent material of fungal cells. The elemental maps confirm that there is a difference in the chemical makeup in the biotemplated (silica and hybrid) samples as compared to the dehydrated samples. Of note, the EDS maps of the trimitic hybrid samples showed a higher concentration of carbon (Figure 5I). This greater amount of carbon likely indicates the presence of more organic material, which is expected since the organic template was not burned off as it was with the silica samples. However, the hybrid samples showed evidence of not being fully biotemplated, with the center of larger trimitic hybrid samples appearing the same as dehydrated samples. While porous, the trimitic sporocarps have sections of very dense packing of hyphae (Figure 4H,I). These dense regions may hamper the infiltration of the acetic acid and silica precursor. The use of a vacuum pump may increase the degree of infiltration, leading to samples with higher levels of silica than were achieved in this study.[45] This lack of infiltration could also be attributed to the proteins that can be found on the outer layer of the fungal cells that make up the hyphal filaments in similar trimitic species which might reduce the adhesion of silica precursors.[46]

FTIR spectra (**Figure 6**) showed distinct similarities and differences between the silica and hybrid samples and differences between the monomitic, dimitic, and trimitic samples for each sample type. The silica and hybrid samples had transmission peaks characteristic of SiO_2 located at ≈1050 cm^{-1}, corresponding to Si—O—Si.[47] Additionally, both sample types included a peak at ≈800 cm^{-1}, indicating the presence of a silanol group, which is the typical terminal group synthesized using TEOS.[47] Both of these peaks were more pronounced in the spectra corresponding to the silica samples (Figure 6A) as compared to those of the hybrid samples (Figure 6B), suggesting the silica samples have a larger SiO_2 content than the hybrid samples. This greater SiO_2 content supports the findings of the EDS maps and corresponding elemental compositions (Table 2). Vibrations associated with O—H stretching, indicated by the peaks at ≈3340 cm^{-1}, were present in all the samples but were more

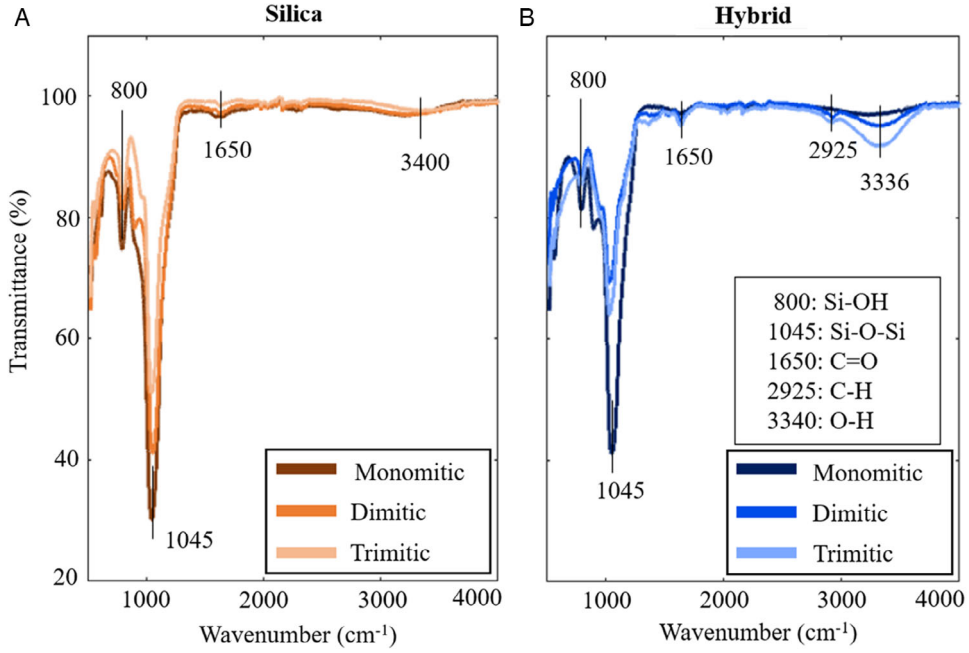

Figure 6. Representative Fourier transform infrared (FTIR) spectra for the monomitic, dimitic, and trimitic samples of the biotemplated samples (silica and hybrid). A) A representative FTIR spectra from a silica sample. B) A representative FTIR spectra from a hybrid sample. Characteristic peaks are labeled with their wavenumber, and the corresponding bonds (shown in the legend in B).

pronounced in the hybrid samples. The hybrid samples also had peaks at ≈2295 cm^{-1}, corresponding to C—H. These same peaks were not present in the silica samples and indicate the presence of residual chitin not burned off during the processing of the hybrid samples.[48]

The silica monomitic, dimitic, and trimitic samples had relatively similar transmittance for the peaks below 2000 cm^{-1}, suggesting a similar formation of SiO_2 networks were formed in each of the samples. However, the silica trimitic samples had the highest transmittance at wavelengths up to 3500 cm^{-1}, suggesting the silica trimitic samples had a lower content of SiO_2 and silanol groups. This may indicate that the trimitic sporocarps are not as well suited to this biotemplating process as the monomitic and dimitic are. The less distinct transmittance peaks above 2000 cm^{-1} of the silica sample FTIR spectra suggest a smaller concentration of organic bonds in these samples as compared to the hybrid samples. This supports the findings of the elemental concentrations of the samples found using EDS, which showed a higher weight percent of the carbon in the hybrid samples.

Of the hybrid samples, the dimitic samples had the most diminished peaks below 2000 cm^{-1}, suggesting that they did not biotemplate as well as the monomitic and trimitic samples. These less pronounced peaks indicate that the SiO_2 did not form networks or crosslink as well as the monomitic or trimitic samples during the biotemplating process. Of note, the silica and hybrid monomitic samples had the most pronounced peaks at ≈1050 cm^{-1}, indicating that the monomitic samples had the best crosslinking and highest concentration of SiO_2 following biotemplating. This lower transmittance indicates that the two biotemplating processes worked best when the monomitic sporocarps were used as an organic template in making the silica and hybrid samples.

TGA showed three distinct characteristic stages of weight loss for the dehydrated sample (**Figure 7**A). Weight loss from room temperature to 200 °C is a result of the evaporation of chemically bonded water molecules.[49] Between 200 and 375 °C, weight loss is attributed to the decomposition of the organic constituents (e.g., chitin). Weight loss between 375 and 500 °C is likely to be the result of further degradation of the residual char, which was supported by the blackened appearance of the dehydrated samples following testing (Figure 7D). The total weight loss of the dehydrated samples by the time the samples reached 500 °C was 87.7%. The silica sample had minimal weight loss (3.3%) attributed primarily to water evaporation, as it occurred mostly in the first 200 °C of the testing and there was no visible change in the appearance of the samples (Figure 7B). The hybrid sample (Figure 7C) showed a total weight loss of 37.6%, close to half of that reported for the dehydrated sample. This result confirms that some of the organic content of the fungal template was replaced in an inorganic silica matrix.

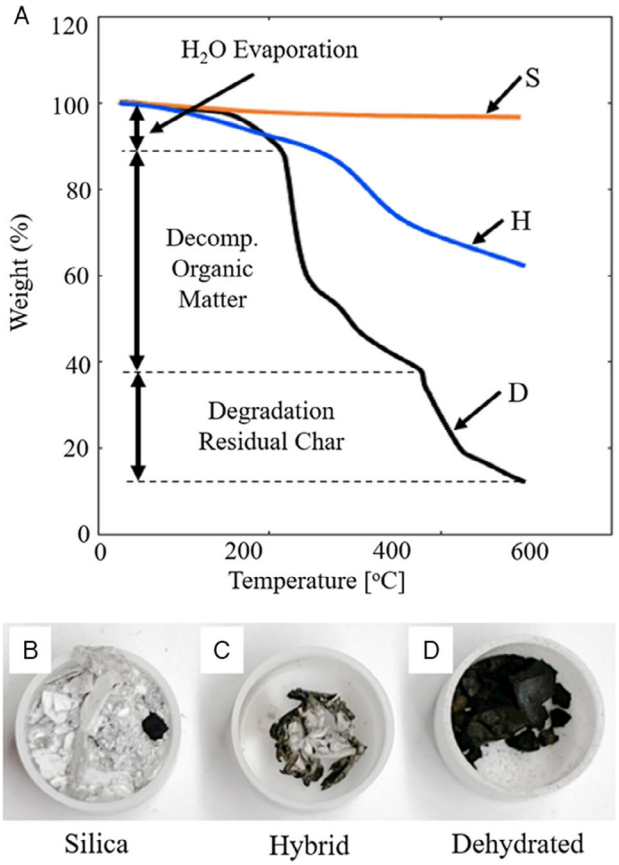

Figure 7. Thermogravimetric analysis (TGA) curves and sample state following testing for monomitic dehydrated (D), silica (S), and hybrid (H) samples.

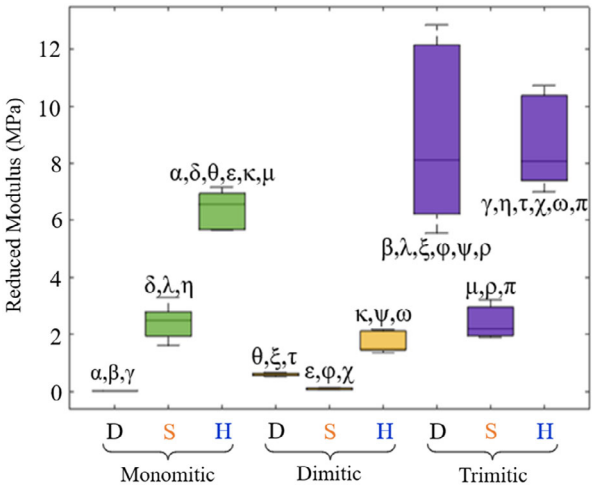

Figure 8. Reduced modulus values of each of the mechanical testing samples (D: Dehydrated, S: Silica, H: Hybrid). Each boxplot represents a sample size of $N = 5$. Matching Greek letters above or below boxplots represent a statistically significant difference where $\alpha = 0.05$.

3.3. Mechanical Properties

Both the reduced modulus and hardness values of the monomitic, dimitic, and trimitic hyphal systems were affected by the different biotemplating processes (**Figure 8** and **9**). Among the biotemplated samples, there was a consistent trend across all three types of hyphal systems that the silica samples had lower average values for the measured mechanical properties (both for

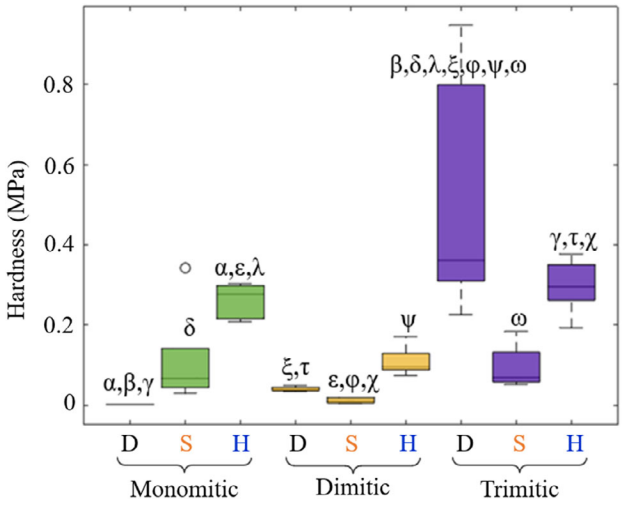

Figure 9. Hardness values of each of the mechanical testing samples (D: Dehydrated, S: Silica, H: Hybrid). Each boxplot represents a sample size of $N = 5$. Matching Greek letters above or below boxplots represent a statistically significant difference where $\alpha = 0.05$.

the reduced modulus and the hardness of the samples) than the hybrid samples. This increase in mechanical resistance is possibly due to the more efficient crosslinking in the hybrid structures (see Section 3.2). Whether this trend yielded statistically significant differences was dependent on both the mechanical property of interest as well as the hyphal system used when biotemplating the samples.

The monomitic samples showed the most statistically significant differences between the different types of samples tested (dehydrated, silica, and hybrid). The average reduced modulus and hardness increased from the dehydrated samples to the silica samples, and then again to the hybrid samples (Figure 8 and 9). There was only a statistically significant difference in both the reduced modulus and hardness values of the monomitic samples between the dehydrated and hybrid samples. The monomitic silica samples achieved an average reduced modulus of more than 126 times larger and an average hardness of more than 73 times larger than the respective averages of the monomitic dehydrated samples. The hybrid samples achieved an average reduced modulus of more than 337 times larger and an average hardness of more than 172 times larger than the respective averages of the monomitic dehydrated samples.

The dimitic samples did not have the same increasing trend in average mechanical properties when comparing the dehydrated samples to the biotemplated samples. Though the differences were not statistically significant, the average reduced modulus and hardness of the dimitic silica samples were smaller than those of the dimitic dehydrated sample (Figure 8 and 9). While both average mechanical properties for the dimitic hybrid samples were larger than both the dimitic dehydrated and silica samples, none of these differences were statistically significant. The dimitic silica samples achieved an average reduced modulus that was roughly 0.2 times as large as and an average hardness about 0.3 times as large as the respective averages of the dimitic dehydrated samples. The hybrid samples achieved an average reduced modulus 2.9 times larger and an average hardness about 2.7 times larger the respective averages of the dimitic dehydrated samples.

Like the dimitic samples, the trimitic samples had the same decrease in the average reduced modulus and hardness values when comparing the dehydrated samples to the silica samples. There was a statistically significant difference in the lower average reduced modulus values of the trimitic silica samples when compared to the larger values of both the trimitic dehydrated and trimitic hybrid samples (Figure 8). When looking at the average hardness values, there was a statistically significant difference between the lower average trimitic silica samples and the trimitic dehydrated samples, but none when compared to the trimitic hybrid samples (Figure 9). There were no statistically significant differences in the average mechanical properties when comparing the trimitic dehydrated samples and the trimitic hybrid samples. The trimitic silica samples achieved an average reduced modulus that was roughly 0.3 times as large as and an average hardness about 0.2 times as large as the respective averages of the trimitic dehydrated samples. The hybrid samples achieved a similar average reduced modulus and an average hardness of more than 0.6 times as large as the respective averages of the trimitic dehydrated samples.

The dehydrated monomitic samples demonstrated the least mechanical resistance of the three dehydrated hyphal structures, which is consistent with previous research.[15] However, the monomitic hybrid samples achieved mechanical resistance with no statistically significant differences when compared to the trimitic dehydrated and hybrid samples, which had the highest average reduced modulus and hardness values (Figure 8 and 9). By using a combination of a sol–gel derived method and a natural hierarchical structure to create the silica and hybrid samples, these monomitic samples achieve higher mechanical properties than either similar silica sol–gel materials or a natural fungal structures.[15,49] The dimitic and trimitic samples did not achieve the same trend of mechanical resistance with the use of biotemplating when compared to the monomitic samples. Chemical analysis completed using FTIR suggested that the dimitic samples did not effectively crosslink, which likely resulted in the lower resistance of the dimitic silica and hybrid samples. The trimitic samples had a higher mechanical resistance than most of the other samples, but the processes of biotemplating did not yield samples with greater mechanical properties that showed a statistically significant difference as compared to the dehydrated samples. This may be in part due to the larger amount of organic template present in the trimitic samples, as was evidenced from EDS data (see Section 3.2). The higher content of natural material would result in mechanical properties that are more indicative of the natural, dehydrated trimitic structures.

3.4. Liquid Absorption Properties

Functional hydrophilic and oleophilic absorption testing indicated that biotemplated samples maintain the functional properties of their organic templates. **Table 3** shows the average absorption of each type of sample for both water and oil absorption tests. The monomitic samples (dehydrated, silica, and

Table 3. Average liquid absorption ($N = 4$ for each average) of the three types of samples (dehydrated, silica, and hybrid) for monomitic, dimitic, and trimitic hyphal systems. The reported absorption is the final weight given as a multiplier of the dry mass of the sample prior to liquid absorption (as a sample with an absorption of 2 weighed twice as much after liquid absorption).

		Absorption	
Hyphal System	Type	Water	Oil
Monomitic	DH	3.8	5.0
	Silica	4.8	4.8
	Hybrid	1.6	1.7
Dimitic	DH	5.1	4.1
	Silica	3.4	4.1
	Hybrid	1.2	1.2
Trimitic	DH	3.1	2.6
	Silica	2.5	2.4
	Hybrid	1.7	1.5

hybrid) consistently absorbed similar amounts of oil and water, as recorded in their separate tests. The trimitic samples (dehydrated, silica, and hybrid) consistently absorbed greater amounts of water. The dimitic biotemplated samples (silica and hybrid) absorbed more oil than water, whereas the dimitic dehydrated samples absorbed more water. There were also trends of absorption based on the type of sample (dehydrated, silica, or hybrid). For each of the hyphal systems (monomitic, dimitic, and trimitic), the hybrid samples absorbed the least amount of liquid and showed statistically significant differences from the dehydrated and silica samples in all cases ($p \leq 5.1$ E-5 for monomitic, $p \leq 4.9$ E-3 for dimitic, and $p \leq 0.03$ for trimitic). For both oil and water, and for each hyphal type, the hybrid samples absorbed less than 1.8 times as much as the weight of the samples. The absorption of the silica samples was more varied and depended on the hyphal system. The monomitic and trimitic silica samples absorbed roughly the same amount of both oil and water: 4.8 and 2.4 times as much as the weight of the samples for the monomitic and trimitic silica samples, respectively. The dimitic silica samples absorbed more oil than water, with absorptions of 4.1 and 3.4 times as much absorption as the weight of the sample, respectively. For each of the hyphal systems, there was no statistically significant difference in the amount of oil the dehydrated and silica samples were able to absorb ($p \geq 0.71$), meaning the silica samples were able to absorb similar amounts of oil as their organic templates. This was not the case for water absorption, where there was a statistically significant difference between the dehydrated and silica samples for only the dimitic and trimitic hyphal systems ($p \leq 0.04$); the monomitic silica samples absorbed similar amounts of water as the dehydrated samples.

The sporocarps produced by fungi are known to be hydrophilic with high moisture contents.[20] Much of this ability to absorb and hold water content may be in part due to the biochemistry of the fungal hyphae,[50] but as is the case for many plant species, capillary forces due to the porous structure of the fungi also play a role.[23] The data from these hydrophilic and oleophilic absorption tests demonstrates that some degree of absorption ability is maintained by mimicking fungal microstructures. By mimicking the microstructure of the natural fungi, the biotemplated samples were able to create a microstructure made up of hollow filaments (Figure 4) that are capable of absorption using capillary forces. Of note, the monomitic silica samples absorbed more water than the monomitic dehydrated samples and absorbed the same amount of oil. While the monomitic hybrid samples absorbed much less water and oil than the monomitic silica and dehydrated samples, they generally absorbed more liquid than the dimitic or trimitic hybrid samples. This decreased ability to absorb the hybrid samples may be due to the loss of porous microstructure created in biotemplating the hybrid samples, which had a greater decrease in porosity than the silica samples (Table 1). Biotemplating the monomitic hyphal structure to create silica samples created the samples with absorption properties close to those of their organic templates.

The ability of the biotemplated samples to absorb liquids demonstrates that these samples maintain some level of the functional properties of the natural sporocarp samples. This is paired with increased mechanical properties, especially in the case of the hybrid samples (see Section 3.3). The different abilities of the biotemplated samples to absorb water and oil make them possible candidates for use in water and oil separation for applications such as the removal of oil contamination. Silica is known as a material that can be oleophilic and can be manufactured to also achieve hydrophobic properties.[51] This combination of being oleophilic and hydrophobic makes silica materials, such as the silica and hybrid samples in this study, prime candidates for inexpensive oil/water filtration materials.[51,52] Additionally, the biotemplated samples in this study are able to outperform the mechanical resistance of other materials that have previously been tested. One such material is aerogels or other sol–gel-derived materials, which are known for their ultra-porous nature and fragile strength.[52–54] Aerogels can be fabricated using similar methods as those used in this study to biotemplate fungi, but lack the added microstructure provided by the hyphal systems of the fungi. While some of these sol–gel materials may be able to absorb more fluid, they have less mechanical resistance than what was achieved in this study.[51,55] The greater mechanical resistance of the materials in this study suggests that they can be used in applications that introduce larger loads, but also that they could potentially be cycled before their mechanical properties begin to degrade.[51] The applications of materials with these functional properties have the potential to aid with environmental remediation.[51,52,56]

In designing and creating materials that may be implemented in environmental remediation, the environmental impact of the manufacturing process and use of the material should be considered. Many materials have been explored in the effort to identify means of filtering oil and water including the use of specialized meshes, silica or copper nanoparticles, nanowire membranes, or aerogels. These materials often require specialized manufacturing to achieve a similar porous or fibrous structure as is seen naturally in filamentous fungi.[52,56] These specialized techniques, expensive materials, or lower mechanical resistances of the resultant structures may inhibit the application of these materials. By biotemplating filamentous fungi using different techniques, filtration materials can be made and tailored to specific applications to achieve the right filtration and mechanical

properties with relatively available and inexpensive materials. Many biotemplating techniques use chemicals and processes that use toxic chemicals that are dangerous to both the user and the environment, but the methods used in this study (Figure 2) use chemicals that are much safer and less toxic than those commonly used in these other biotemplating processes.[25,26,30] Additionally, the chemical makeup of the biotemplated samples (silica and silica-chitin hybrid) contain materials found naturally in the environment, though the future study may be completed to better understand the full environmental impact of these materials on different environments.

The greater ability of the monomitic hyphal structures to be biotemplated may be a result of the microstructure being composed of only one type of hyphae. Monomitic filamentous fungi (such as those in the *Agaricomycetes* class of Fungi) only have generative hyphae. These hyphae have thinner cell walls than the other two types of hyphae that are found in dimitic and trimitic fungi.[57,58] While in fresh or dehydrated monomitic samples, the lack of additional hyphal types results in a weaker structure than what is found in dimitic or trimitic samples,[15] it appears that the lack of additional hyphae improves the efficacy of the biotemplating processes. Additionally, monomitic sporocarps (such as white, oyster, or shiitake mushrooms) are more commonly available commercially at a lower cost than dimitic or trimitic fungi, making them a cost-effective choice for an organic template.

4. Conclusions

This study characterized the structure, chemical makeup, mechanical properties, and functional properties of silica and silica-chitin hybrid samples that mimic the microstructure of monomitic, dimitic, and trimitic fungi. Using these methods and analysis of their individual results lead to the following conclusions: 1) Biotemplated samples using the methods in this study are able to capture and mimic the natural structures found in fungal sporocarps. The porous, filamentous structure of the sporocarps was copied in the silica and hybrid samples, though there was a decrease in the porosity of the samples, with the hybrid samples being the least porous. 2) The silica and hybrid samples achieved distinct chemical compositions from the dehydrated fungal sporocarps. Biotemplating led to the introduction of silica, and the reduction of carbon in these samples. The silica samples achieved the highest levels of silica, while analysis showed that hybrid samples maintained some amount of carbon, likely an artifact from the acetic acid used as well as the chitin present in the organic template. 3) Hybrid samples achieved greater mechanical resistance than silica samples on average. While the actual values of the reduced modulus and hardness depended on the hyphal system used to create the samples, this trend was consistent. The silica and hybrid samples only resulted in mechanical resistance greater than the dehydrated sporocarp samples in the case of the monomitic samples. 4) Silica and hybrid samples maintain some degree of the ability to absorb liquids, which is common to natural fungal sporocarps. Silica samples absorbed the greatest amount of liquid, with the monomitic samples outperforming the overall absorption seen in dimitic and trimitic samples. This ability to absorb both oil and water to different degrees makes these sample a possible candidate for use in environmental remediation. 5) Monomitic samples offer the best option as a template for biotemplated samples, as they are the most cost-effective and provide the greatest increase in mechanical resistance and maintenance of absorption properties when biotemplated.

Conflict of Interest

The authors declare no conflict of interest.

Data Availability Statement

The data that support the findings of this study are available from the corresponding author upon reasonable request.

Keywords

absorption material, bioinspiration, biotemplating, fungi

Received: June 28, 2022
Revised: August 22, 2022
Published online:

[1] T. Niskanen, B. Douglas, P. Kirk, P. Crous, R. Lücking, P. B. Matheny, L. Cai, K. Hyde, M. Cheek, *State World's Fungi 2018*, Royal Botanic Gardens, Kew, Richmond, United Kingdom **2018**, pp. 18–23.
[2] M. Cheek, E. N. Lughadha, P. Kirk, H. Lindon, J. Carretero, B. Looney, B. Douglas, D. Haelewaters, E. Gaya, T. Llewellyn, A. M. Ainsworth, Y. Gafforov, K. Hyde, P. Crous, M. Hughes, B. E. Walker, R. C. Forzza, K. M. Wong, T. Niskanen, *Plants People Planet* **2020**, *2*, 371.
[3] D. L. Hawksworth, R. Lücking, *Microbiol. Spectrum* **2017**, *5*, 5.
[4] Y. C. Fung, *Biomechanics: Mechanical Properties of Living Tissues*, Springer, New York, NY **1981**.
[5] N. P. Money, *Mycologist* **2004**, *18*, 71.
[6] L. Yafetto, D. J. Davis, N. P. Money, *Fungal Genet. Biol.* **2009**, *46*, 688.
[7] N. P. Money, *Fungal Biol. Rev.* **2008**, *22*, 71.
[8] R. R. Lew, in *Biology of the Fungal Cell* (Eds: D. Hoffmeister, M. Gressler), Springer International Publishing, Cham **2019**, pp. 83–94.
[9] N. P. Money, in *Biology of the Fungal Cell* (Eds: R. J. Howard, N. A. R. Gow), Springer, Berlin, Heidelberg **2001**, pp. 3–17.
[10] N. P. Money, M. W. F. Fischer, in *Plant Relationships* (Ed: H. B. Deising), Springer, Berlin, Heidelberg **2009**, pp. 115–133.
[11] D. L. Porter, A. J. Bradshaw, R. H. Nielsen, P. Newell, B. T. M. Dentinger, S. E. Naleway, *J. Mech. Behav. Biomed. Mater.* **2022**, *125*, 104934.
[12] C. Müller, S. Klemm, C. Fleck, *Appl. Phys. A* **2021**, *127*, 178.
[13] L. Zhao, D. Schaefer, H. Xu, S. J. Modi, W. R. LaCourse, M. R. Marten, *Biotechnol. Prog.* **2005**, *21*, 292.
[14] S. M. Stocks, C. R. Thomas, *Biotechnol. Bioeng.* **2001**, *73*, 370.
[15] D. L. Porter, S. E. Naleway, *Acta Biomater.* **2022**, *145*, 272.
[16] Y. Xing, M. Brewer, H. El-Gharabawy, G. Griffith, P. Jones, *IOP Conf. Ser. Earth Environ. Sci.* **2018**, *121*, 022032.
[17] G. A. Holt, G. Mcintyre, D. Flagg, E. Bayer, J. D. Wanjura, M. G. Pelletier, *J. Biobased Mater. Bioenergy* **2012**, *6*, 431.
[18] M. Jones, A. Mautner, S. Luenco, A. Bismarck, S. John, *Mater. Des.* **2020**, *187*, 108397.
[19] S. M. Bowman, S. J. Free, *BioEssays* **2006**, *28*, 799.

[20] R. Fogel, *Can. J. Bot.* **1976**, *54*, 1152.
[21] L. Cabral, C. R. F. S. Soares, A. J. Giachini, J. O. Siqueira, *World J. Microbiol. Biotechnol.* **2015**, *31*, 1655.
[22] V. Göhre, U. Paszkowski, *Planta* **2006**, *223*, 1115.
[23] W. F. Pickard, *Prog. Biophys. Mol. Biol.* **1981**, *37*, 181.
[24] O. Paris, G. Fritz-Popovski, D. V. Opdenbosch, C. Zollfrank, *Adv. Funct. Mater.* **2013**, *23*, 4408.
[25] A. S. Deshpande, I. Burgert, O. Paris, *Small* **2006**, *2*, 994.
[26] A. Temiz, N. Terziev, B. Jacobsen, M. Eikenes, *J. Appl. Polym. Sci.* **2006**, *102*, 4506.
[27] A. Aygün, S. Özdemir, M. Gülcan, K. Cellat, F. Şen, *J. Pharm. Biomed. Anal.* **2020**, *178*, 112970.
[28] C. Zollfrank, P. Cromme, M. Rauch, H. Scheel, M. H. Kostova, K. Gutbrod, S. Gruber, D. Van Opdenbosch, *Bioinspired, Biomimetic Nanobiomater.* **2012**, *1*, 13.
[29] A. M. Fontes, R. Geris, A. V. dos Santos, M. G. Pereira, J. G. S. Ramalho, A. F. da Silva, M. Malta, *Biomater. Sci.* **2014**, *2*, 956.
[30] D. V. Opdenbosch, G. Fritz-Popovski, W. Wagermaier, O. Paris, C. Zollfrank, *Adv. Mater.* **2016**, *28*, 5235.
[31] M. Mroz, M. Ali, J. Howard, K. Carlson, S. E. Naleway, *JOM* **2021**, *73*, 1736.
[32] "Index Fungorum - Search Page," http://www.indexfungorum.org/Names/Names.asp (accessed: August 2021).
[33] R. L. Berendsen, S. I. C. Kalkhove, L. G. Lugones, H. A. B. Wösten, P. A. H. M. Bakker, *Environ. Microbiol. Rep.* **2012**, *4*, 227.
[34] A. M. Vos, R.-J. Bleichrodt, K. C. Herman, R. A. Ohm, K. Scholtmeijer, H. Schmitt, L. G. Lugones, H. A. B. Wösten, *Environ. Microbiol.* **2021**, *23*, 224.
[35] O. Miettinen, E. Larsson, E. Sjökvist, K.-H. Larsson, *Cladistics* **2012**, *28*, 251.
[36] M. L. Gargano, G. I. Zervakis, O. S. Isikhuemhen, G. Venturella, R. Calvo, A. Giammanco, T. Fasciana, V. Ferraro, *Diversity* **2020**, *12*, 230.
[37] D. N. Pegler, *Mycol. Res.* **1996**, *100*, 129.
[38] F. Hennicke, Z. Cheikh-Ali, T. Liebisch, J. G. Maciá-Vicente, H. B. Bode, M. Piepenbring, *Phytochemistry* **2016**, *127*, 29.
[39] X.-C. Wang, R.-J. Xi, Y. Li, D.-M. Wang, Y.-J. Yao, *Plos One* **2012**, *7*, e40857.
[40] D.-W. Li, *Laboratory Protocols in Fungal Biology*, Cham, Switzerland **2013**.
[41] G. Qin, J. Liu, B. Cao, B. Li, S. Tian, *Plos One* **2011**, *6*, e21945.
[42] K. B. Aslanidi, M. A. Tsyganov, A. E. Ivanova, T. A. Belozerskaya, G. R. Ivanitskii, *Dokl. Biochem. Biophys.* **2007**, *413*, 47.
[43] G. M. Sapers, R. L. Miller, S.-W. Choi, P. H. Cooke, *J. Food Sci.* **1999**, *64*, 889.
[44] K. Baskaran, M. Ali, K. Gingrich, D. L. Porter, S. Chong, B. J. Riley, C. W. Peak, S. E. Naleway, I. Zharov, K. Carlson, *Microporous Mesoporous Mater.* **2022**, *336*, 111874.
[45] C. Martos, F. Rubio, J. Rubio, J. L. Oteo, *J. Sol-Gel Sci. Technol.* **2003**, *26*, 511.
[46] M. Haneef, L. Ceseracciu, C. Canale, I. S. Bayer, J. A. Heredia-Guerrero, A. Athanassiou, *Sci. Rep.* **2017**, *7*, 41292.
[47] M. Heidari Nia, R. Koshani, J. G. Munguia-Lopez, A. R. Kiasat, J. M. Kinsella, T. G. M. van de Ven, *ACS Appl. Bio Mater.* **2021**, *4*, 4201.
[48] T. Y. A. Essel, A. Koomson, M.-P. O. Seniagya, G. P. Cobbold, S. K. Kwofie, B. O. Asimeng, P. K. Arthur, G. Awandare, E. K. Tiburu, *Polymers* **2018**, *10*, 466.
[49] M. Jones, T. Bhat, E. Kandare, A. Thomas, P. Joseph, C. Dekiwadia, R. Yuen, S. John, J. Ma, C.-H. Wang, *Sci. Rep.* **2018**, *8*, 17583.
[50] Y. Duan, S. C. Jana, B. Lama, M. P. Espe, J. Non-Cryst, *Solids* **2016**, *437*, 26.
[51] D. R. Olicón-Hernández, J. González-López, E. Aranda, *Front. Microbiol.* **2017**, *8*, 1792.
[52] R. Kumar Gupta, G. J. Dunderdale, M. W. England, A. Hozumi, *J. Mater. Chem. A* **2017**, *5*, 16025.
[53] Z. Xue, Y. Cao, N. Liu, L. Feng, L. Jiang, *J. Mater. Chem. A* **2014**, *2*, 2445.
[54] N. T. Cervin, C. Aulin, P. T. Larsson, L. Wågberg, *Cellulose* **2012**, *19*, 401.
[55] H. Sehaqui, M. Salajková, Q. Zhou, L. A. Berglund, *Soft Matter* **2010**, *6*, 1824.
[56] A. Venkateswara Rao, N. D. Hegde, H. Hirashima, *J. Colloid Interface Sci.* **2007**, *305*, 124.
[57] X. Yue, Z. Li, T. Zhang, D. Yang, F. Qiu, *Chem. Eng. J.* **2019**, *364*, 292.
[58] P. Kirk, P. Cannon, D. Minter, J. Stalpers, *Dictionary of the Fungi*, CABI Publishing, Wallingford **2008**.